In Situ Photopolymerization of PEGDA-Protein Hydrogels on Nanotube Surfaces

Evan M. Smoak, Marsiyana M. Henricus, Ipsita A. Banerjee

Department of Chemistry, Fordham University, Bronx, NY 10458

ABSTRACT: Peptide nanotubes were used as templates for the growth of poly(ethylene glycol) diacrylate-based nanoscale hydrogels via photopolymerization. A Rose Bengal di-amine derivative comprised of a photoactivator and coinitiator within the same molecule was used as the photoinitiator to increase photopolymerization efficiency. The nanotubes were covalently bound to the protein BSA before formation of the hydrogels. We also examined the photopolymerization efficiency in reactions involving nanotubes in the absence of BSA. Although photopolymerization occurred efficiently under both conditions, higher yields of highly crosslinked nanostructures were obtained for the protein bound nanotube-PEGDA hydrogels. It was observed that the swelling ratios were also dependent upon whether or not BSA was bound to the nanotubes before photopolymerization. The thermal properties of the nanocomposite hydrogels were investigated using differential scanning calorimetry analyses and the morphologies were examined using TEM, SEM, and AFM analyses. Such nanocomposites prepared by low cost, mild methods could be extremely efficient for the *in situ* preparation of three-dimensional arrays of peptide nanotube grafted hydrogels. © 2010 Wiley Periodicals, Inc. J Appl Polym Sci 118: 2562–2571, 2010

Key words: photopolymerization; BSA; hydrogels; nanotubes

INTRODUCTION

Over the past decade, substantial research has been conducted toward the design and fabrication of a variety of polymeric micro- and nanostructured materials with tailored functional properties for desired applications.[1–7] To enhance their applications, surface modification of the nanostructures is often carried out.[8–13] Although a variety of procedures have been used for the preparation of such nanostructures, difficulties associated with their production have limited their wide applicability. In lieu of this, development of hybrid biomaterials based on blends of synthetic and biological polymers have attracted much attention.[14–20] Such hybrid biomaterials combine the strong mechanical properties of synthetic polymers with the biocompatibility of biological polymers, such as proteins, DNA, and natural polysaccharides.[21–27] Their distinctive features can be utilized in controlled release, bioencapsulation, catalysis, biosensors, and in packaging.[28–33] In particular, nanoscale polymeric hydrogels have gained considerable attention in recent years as one of the most promising drug delivery systems because of the combination of nanoparticulate size and the characteristics of hydrophilicity and high water content, which allows for permeability to ions and metabolites and makes them more favorable for biotolerance.[34,35]

In general, hydrogel nanoparticles have immense potential in various applications, such as implant materials, contact lenses, tissue engineering, biomarkers, wound dressing, and as drug supports for controlled release.[36–45] Several polymeric hydrogel nanoparticulate systems have been prepared and characterized. Particularly some synthetic polymers based on polyvinyl alcohol, polyethyleneimine, polyvinyl pyrrolidone, polyethylene glycol, polyacrylic acid, and poly-*N*-isopropylacrylamide have been reported with different characteristics and features with respect to drug delivery.[46–54] In particular, polyethylene glycol has been combined with several bioactive polymers, such as hyaluronic acid, lactides, alginate, and poly(ε-caprolactone) to create interpenetrating polymer networks for a range of biomedical applications.[55–59] Recently, thiolated gelatin nanoparticles were modified with poly(ethylene glycol) (PEG) chains for targeting breast cancer cells.[60] Such nanoparticulate systems may be potentially used to target encapsulated drugs and genes to tumors. Protein-*graft*-PEG hydrogels have also shown cell adhesiveness and mechanical strength, which is promising particularly with respect to applications in tissue regeneration.[61] Photocrosslinkable oligo[poly(ethylene glycol) fumarate] hydrogels have been used to encapsulate chondrocytes, for

applications in cartilaginous tissue engineering.[62] Multifunctional bovine serum albumin (BSA)-amplified PEG-NH$_2$ nanogels have been utilized in designing protein chips for biosensors.[63]

To construct nanoscale hydrogels with controlled morphologies, researchers have frequently used templating approaches as well. For example, liposomes have also been used to synthesize nanoscale hydrogels consisting of PEG-diacrylate (PEG-DA) via photopolymerization.[64] Carbon nanotubes have also been functionalized with PEG in the presence of specific antibodies to enhance biocompatibility and specific biomolecular recognition, while at the same time reducing nonspecific protein adsorption.[65] Peptide polymer hybrid nanotubes were recently constructed using cyclic peptides modified with specific chemical groups at distinct side-chain positions, which served as initiation sites for controlled free-radical polymerization.[66] Although a myriad of research has been carried out using lipid, polymer vesicles, and surfactants as templates for polymer immobilization, to our knowledge immbolization of hydrogels on self-assembled peptide nanotubes via direct photopolymerization on peptide nanotube surfaces is yet to be explored. Peptide and lipid-based nanotubes display several properties that make them desirable biomaterial candidates, including facile self-assembly and adaptablity to functionalization for improved biocompatibility.[67–74] Designing a system that involves functionalizing peptide nanotubes with PEGDA-crosslinked with proteins is likely to lead to novel biomaterials and may facilitate in developing miniature biodevices for drug delivery and tissue engineering applications.

In this work, we have photopolymerized PEGDA on self-assembled peptide nanotube surfaces in the presence of visible light. The photopolymerization was carried out in the presence of Rose Bengal di-*n*-butylamine as the photoinitiator either directly on the nanotube surfaces, or after the nanotubes were bound to BSA. The Rose Bengal di-*n*-butylamine derivative combines the xanthene dye moiety photoactivator and coinitiator system within a single molecule, thus attenuating the reaction kinetics and enhancing photopolymerization efficiency. It is well known that albumin use as a covering agent (either as adsorbed, crosslinked, or covalently attached) onto the surface of a biomaterial, increases the biocompatibility of the material mainly by reducing platelet adhesion.[75] Thus, the formation of PEGDA-hydrogels on nanotube surfaces would be very significant. The formation of the hydrogels was confirmed by spectroscopic methods and the morphologies and thermal properties of the nanotube-based hydrogels were investigated. Such nanoscale hydrogels could be prepared with a wide range of proteins bound to the nanotubes and could lead to a new family of nanoscale hydrogels having potential applications for controlled release devices, tissue engineering and wound dressing materials.

EXPERIMENTAL

Materials

Albumin from bovine serum minimum (98% electrophoresis grade), poly(ethylene glycol) diacrylate, L-phenylalanine benzyl ester hydrochloride, di-*N*-butylamine, Rose Bengal, dibromoethane, 1-hydroxy-benzotriazole hydrate (HoBt), *N*-(3-dimethyl-aminopropyl)-*N'*-ethyl-carbodiimide hydrochloride (EDAC), azelaic acid, solvents, such as dimethylformamide, silica gel, tetrahydrofuran, methanol, triethylamine, buffers of various pH values were purchased from Sigma Aldrich and used as received.

Methods

Synthesis of the bolaamphiphile and self-assembly of nanotubes

To prepare template nanotubes for the incorporation of PEGDA and proteins, the bolaamphiphile bis(*N*-a-amido-phenylalanine)-1,7-heptane dicarboxylate ($1.0 \times 10^{-3}M$) was synthesized and self-assembled into nanotubes at pH 4 over a period of 2 weeks. The bolaamphiphile peptide monomer was synthesized according to previously established methods and the details of the synthesis and the self-assembly process are described elsewhere.[76–78] Briefly, the bolaamphiphile was synthesized by coupling the benzyl ester of the amino acid, phenylalanine (1.2 g) with the appropriate diacarboxylic acid (0.65 g) (azelaic acid) at $0-3°C$ in dimethylformamide (DMF) in the presence of EDAC and 1-hydroxy-benzotriazole, which were used as coupling agents and as additives, respectively. After 24 h, the DMF was rotary evaporated and the intermediate obtained was filtered and washed with citric acid (0.1*M*) and sodium bicarbonate solutions (0.1*M*). The intermediate was then recrystallized using DMF. Finally, the ester groups were deprotected by base hydrolysis with NaOH at 96°C. The product obtained was recrystallized using a mixture of 50–50 mixture of ice-cold water and acetone and utilized for the growth of nanotubes. After the formation of nanotubes over a 2–3 week period, the nanotubes were sonicated, washed with nanopure water, and centrifuged thrice before reaction with BSA and subsequent photopolymerization reactions.

Preparation of Rose Bengal di-*n*-butylamine derivative

The Rose Bengal di-*n*-butylamine derivative was synthesized according to previously established

methods.[79] Briefly, Rose Bengal was coupled with dibromoethane to form the intermediate 2′-bromo-ethylester in the presence of DMF as a solvent. The materials were refluxed at 50°C for 96 h and the formed product was rotary evaporated to remove the solvent under vacuum and recrystallized using methanol and dried thoroughly. It was then allowed to react with di-N-butyl amine in DMF in the presence of potassium carbonate (0.1M) and the reaction was allowed to stir for 48 h at room temperature. The formation of the product was followed by TLC. After the solvent was removed, the formed RB-di-N-amine derivative, was purified by silica gel column chromatography. The fractions containing the product were combined and rotary evaporated to obtain the final product, which was confirmed by ^{1}H-NMR spectroscopy. ^{1}H-NMR DMSO-d_6 spectrum showed peaks at δ 0.9 (t, 6H), 1.4 (m, 8H), 2.9 (t, 4H), 3.1 (t, 4H), 4.2 (t, 2H), 7.3 (s, 1H), 7.6 (s, 1H). Elemental analysis calculated for $C_{30}H_{25}Cl_4I_4NO_5O_5$: C 31.87; H 2.52; Cl 12.56, N, 1.24, I 44. 63, O 7.18; Found: C, 31.96%, H, 2.25%, Cl 11.96%, I 45.31%, N 1.50%, and O 7.02%

Derivatization of nanotubes with BSA

To 200 μL of self-assembled nanotube solution, 0.1M NHS (100 μL) and 0.25M EDAC (150 μL) were added in order to activate the carboxylate groups of the nanotubes. The reaction mixture was vortexed for an hour, followed by the addition of 300 μL of 0.01 mM BSA at pH 7. The solution was incubated overnight at 4°C and vortexed to ensure covalent binding between the nanotubes and the protein. The protein bound nanotubes were then washed thrice with nanopure water and centrifuged to remove any unbound protein. The incorporation of the protein on the nanotube surface was confirmed by FTIR spectroscopy.

Attachment of Rose Bengal di-n-butylamine derivative to protein bound nanotubes

It is well known that proteins such as BSA have a high affinity for dye molecules and can efficiently bind to them via noncovalent interactions.[80–82] The protein bound nanotubes were incubated with 200 μL of 0.1M solution of Rose Bengal di-n-butyl amine at pH 7. The samples were incubated for 48 h, in the dark at 4°C. The reaction mixtures were then washed thrice with nanopure and centrifuged to remove any unbound photoinitiator. The incorporation of the photoinitiator on the nanotube surface was confirmed by absorbance as well as fluorescence spectroscopy. As a control experiment, 200 μL of 0.1 mM RBN solution in THF was prepared and added 200 μL of self-assembled nanotube solutions (which were not bound to BSA) and incubated for 48 h, in the absence of BSA. The solutions were then washed and centrifuged and the incorporation of photoinitiator was confirmed by spectroscopic methods.

Hydrogel formation via photopolymerization

To investigate the efficacy of formation of the hydrogel on the nanotubes, 200 μL of 25% w/v solution of PEGDA (MW 575 Da) were added to 200 μL protein-photoinitiator-bound nanotubes for the photopolymerization reactions in pyrex tubes. The pH of the reaction mixture was adjusted to 7.0. The samples were illuminated with two 90W lamps (light emitted between 380 and 510 nm) spaced 5 cm away from the sample on either side. The samples were bubbled with nitrogen for 20 min, before illumination to remove oxygen from the reaction environment as well continuously bubbled with nitrogen through out the reaction. The samples were irradiated for varying periods of time, up to a maximum of 30 min and the efficacy of product formation was confirmed by the weights of the gels obtained after drying the samples. Similar procedure was carried out with dye bound nanotubes (in the absence of BSA) as a control.

Swelling studies

The swelling kinetics of the nanotube bound hydrogels were measured over a period of 24 h days at room temperature. The nanotube bound hydrogels were dried at 40°C in the oven for 24 h before carrying out swelling studies. The dried samples were weighed and immersed in 15 mL of a phosphate-buffered saline buffer solution at room temperature for predetermined periods; they were then removed, and surface water was blotted by the filter paper and weighed until there was no further weight change. The equilibrium swelling ratio (Q_e) was calculated as follows: $Q_e = [(W_s - W_d)/W_d] \times 100\%$ where W_s is the weight of the swollen hydrogel at time t and W_d is the weight of the dry hydrogel at $t = 0$.

Evaluation of release of BSA from hydrogel nanotubes

Even though the BSA was covalently bound to the nanotube surfaces prior to photopolymerization, we examined the possibility of BSA leaching out of the hydrogels after the reaction. For this study, the formed hydrogel nanotubes were suspended in 5 mL solution of pH 7.4 buffer for varying periods of time. The solutions were then centrifuged and the contents of the supernatants were evaluated by Bradford method to examine the presence of BSA content.

Characterization

Scanning electron microscopy

The morphology of the samples obtained after irradiation was examined by by SEM (Hitachi S-2600N) operated at 25 kV. The washed samples were dried and carbon coated before analysis.

FTIR spectroscopy

To confirm the incorporation of PEGDA, as well as the proteins, on to template nanotubes, FTIR analyses were performed using IR DIGILAB, Excali-BuvHE Series FTS 3100. The samples were dried at room temperature and mixed with KBr to make pellets and then analyzed. All spectra were taken at 4 cm^{-1} resolution with 100 scans taken for averaging.

Absorbance spectroscopy

Absorbance spectroscopy measurements were carried out using Varian Cary3 UV/Visible spectrophotometer with Varian data analysis tools at a range of 400–800 nm wavelengths. All measurements were carried out in aqueous solutions.

Fluorescence spectroscopy

Fluorescence spectroscopy was used to confirm the incorporation of the photoinitiator on the nanotubes in the absence and presence of the proteins. Fluorescence spectra were taken using Jobin Yvon Fluoromax 3 fluorescence spectrometer in a wavelength range of 570–800 nm, excited at 557 nm.

Atomic force microscopy

AFM analyses were carried out using a Quesant Universal SPM in tapping mode in air using silicon nitride tips.

Differential scanning calorimetry

To examine the thermal properties of the hydrogel nanotubes obtained by photopolymerization, differential scanning calorimetry (DSC) analyses were carried out using Universal V4.3A from TA Instruments differential scanning calorimeter. The measurements were carried out at temperature range between –60 and 250°C. The heat flow rates were recorded at a rate of 5°C per minute under nitrogen atmosphere. These measurements provide quantitative and qualitative information about physical and chemical changes that involve endothermic and exothermic processes.

RESULTS AND DISCUSSION

The bis(*N*-α-amido-Phe)-1,7-heptane dicarboxylate bolaamphiphile was synthesized and self-assembled according to previously established methods.[77] In general, the nanotubes formed by self-assembly at room temperature within a period of two weeks at pH 4. The bolaamphiphiles are pH sensitive because of the presence of the free carboxyl groups. In general, both hydrogen-bonding interactions between the amide and carboxyl groups as well as the hydrophobic and stacking interactions between the phenylalanine moieties allowed for the facile self-assembly of the nanotubes. It has been observed that such assemblies are promoted by protonation and/or hydrophobic interactions between the peptide moieties.[83] The self-assembled nanotubes were sonicated, centrifuged, and washed thoroughly with nanopure water. The nanotubes were then covalently bound to BSA before treatment with the photoinitator to carry out the photopolymerization reactions. The covalent binding between nanotubes and the proteins occurs efficiently between the free lysyl amino groups of the BSA[84] and the free carboxylate groups of the nanotubes. The carboxylic acid groups of the nanotubes were activated using EDAC and NHS and allowed to react with BSA. After reaction the samples were washed and centrifuged to remove any unbound protein. The incorporation of the proteins was confirmed by FTIR spectroscopy. Because Rose Bengal has a high affinity for BSA,[85] and proteins in general, the photoinitiator RBN was then incubated with the protein bound nanotubes, washed and centrifuged before carrying photopolymerization reactions for different periods of time. The scheme for fabrication of the PEGDA hydrogel bound nanotubes is shown in Figure 1.

On average, the tubular structures used were 100–200 nm in diameter. Figure 2 shows SEM images that indicate the morphologies of the nanotubes before and after photopolymerization. Figure 2(a) shows a SEM image of a self-assembled nanotube with smooth surface, whereas Figure 2(b) shows the SEM image of nanotubes after photopolymerization after 5 min of irradiation. Figure 2(c) shows the SEM image of PEG-diacrylate photopolymerized on BSA-bound nanotubes after 15 min of irradiation. Upon comparison of the nanotubes before reaction [Fig. 2(a)] and after incorporation of PEGDA [Figure 2(b,c)], there is a significant difference observed on the surface of the tubes. These SEM images show distinct, though uneven, network structures forming a highly intertwined mesh indicating the formation of the hydrogel on the nanotube surfaces. We did not observe any difference in the morphology of the structures formed after 15 min of irradiation. Further the viscosity of the sample did not change beyond 15 min of irradiation. This indicates that photopolymerization was essentially complete within 15 min of irradiation.
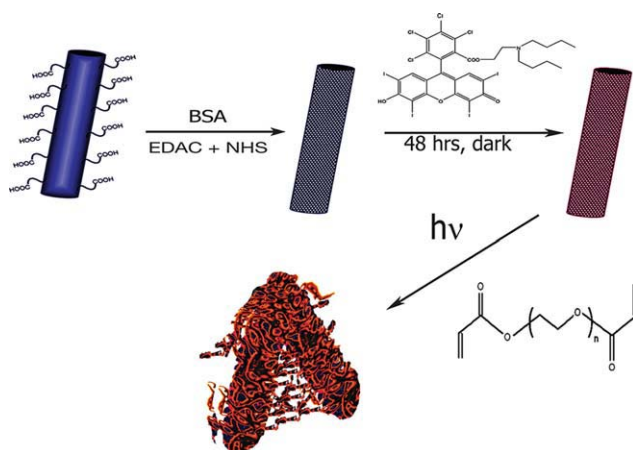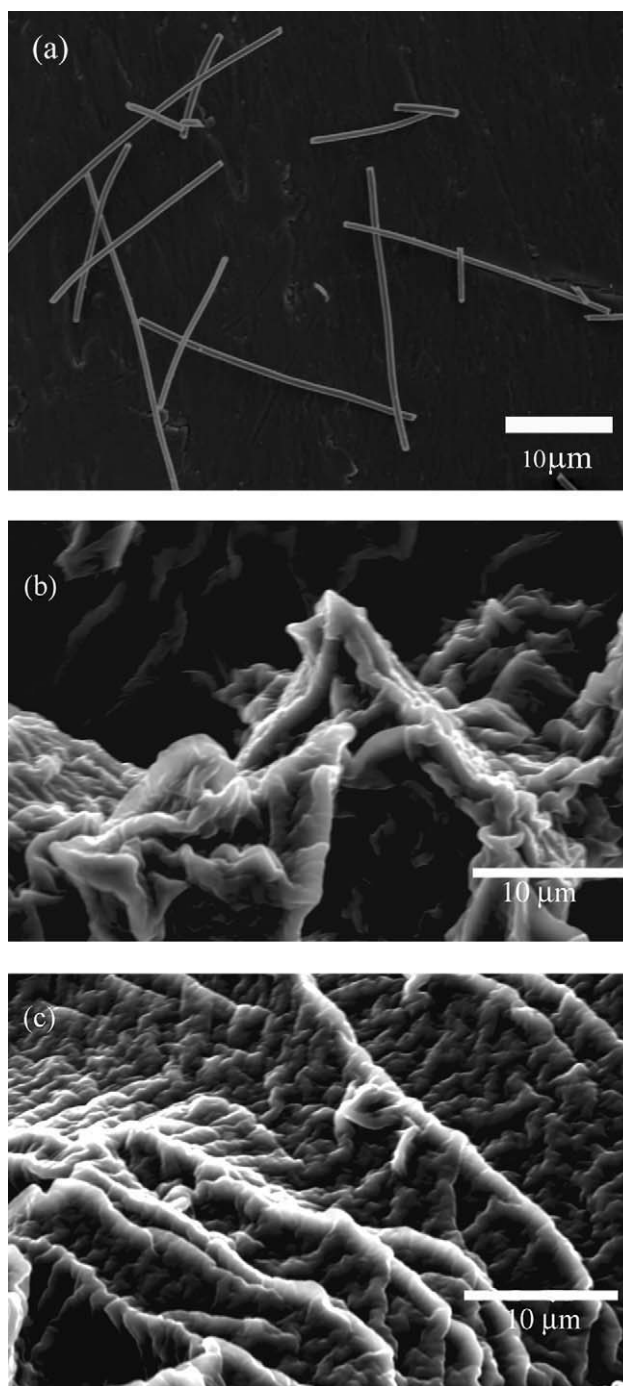
Figure 1 Scheme for formation of PEGDA hydrogels on BSA bound nanotubes. [Color figure can be viewed in the online issue, which is available at www.interscience.wiley.com.]

Photopolymerization experiments were conducted on nanotubes incubated with the dyes directly, without prior binding with BSA as well. It is expected that the peptide nanotubes, which contain phenylalanine moieties, would noncovalently interact with the xanthene moiety of the RBN photoinitator by hydrophobic interactions and promote noncovalent binding. Further, the carboxylate groups, have an affinity toward the tertiary amine group of the photoinitiator. Upon photopolymerization, with the nanotubes (which were not bound to BSA prior to incorporation of the photoinitiator) directly, relatively distinct structures were observed. The AFM images shown in Figure 3 clearly indicate a change in the roughness of the surfaces of the nanotubes. Figure 3(a) AFM amplitude image of bare nanotubes after incubating with RBN, whereas Figure 3(b) shows the AFM image after irradiation with PEGDA. As seen in Figure 3(b), there is a distinct difference in the surface of the nanotubes and PEGDA hydrogels were formed directly on the surface of the nanotubes, though no mesh was observed. These results indicate that the Rose Bengal di-*n*-butyl amine photoinitiator effectively photopolymerized PEGDA on the nanotube surfaces.

Xanthene dye-coinitiator systems (particularly in intermolecular electron transfer reaction systems) are common visible light radical forming systems and have been used as photopolymerization initiators in the past.[86–88] Recently, PEGDA hydrogels were photopolymerized on glass and silicon surfaces in the presence of the xanthene dye eosin and triethanol amine was used as the coinitiator.[89] Relatively less attention has been paid to the direct role of intramolecular electron transfer reactions. In the photoinitiator that we have used for the preparation of the nanotube bound hydrogels, a donor–acceptor complex consisting of a xanthene dye and the reductant moiety are incorporated within a single molecule to enhance the reactiv-

ity of the photoinitiator by intramolecular photoinduced electron transfer. This strategy has some obvious advantages compared with the use of an intermolecular reaction system for the generation of radicals. Primarily, one can avoid the use of high quantity of reductants, which may not be compatible with the components of the reaction mixture and

Figure 2 (a) SEM image of self-assembled peptide nanotubes; (b) SEM image of PEGDA immobilized on BSA-bound peptide nanotubes after 5 minutes of irradiation; (c) SEM image of PEGDA immobilized on BSA-bound peptide nanotubes after 15 minutes of irradiation.
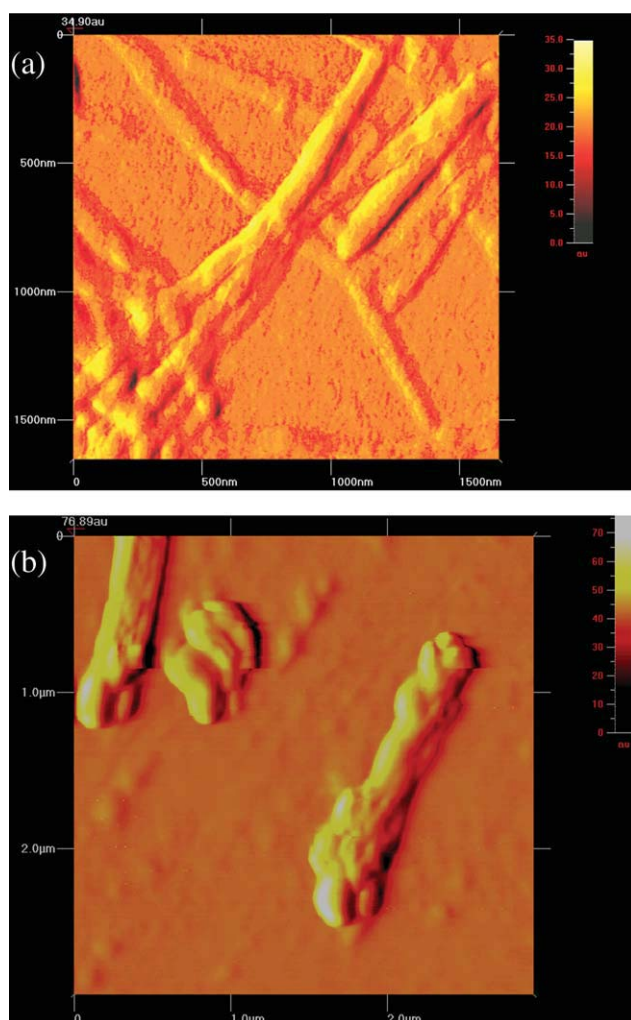
Figure 3 (a) AFM amplitude image of peptide nanotubes bound to photoinitiator RBN; (b) AFM amplitude image of PEGDA photopolymerized directly on nanotube surfaces. [Color figure can be viewed in the online issue, which is available at www.interscience.wiley.com.]

further, reduce back electron transfer, thus leading to efficient photopolymerization on the nanotube surfaces. As seen in Figures 2 and 3, when the nanotubes were bound to BSA before irradiation with the photoinitiator, higher quantities of intertwined crosslinked networks are observed compared with those obtained on nanotubes without BSA. This is most likely because in addition to the photoinitiator, an electron or hydrogen atom transfer may also be occurring from BSA to the dye moiety or some of the protein itself may be crosslinked on the nanotube surfaces, leading to the highly intertwined mesh.[90,91] Further investigations on the exact mechanism for photocrosslinking is ongoing and will be published separately.

FTIR analysis

Figure 4 shows a comparison of the FTIR spectra of nanotubes before and after photopolymerization.

Figure 4(a) shows the spectrum of nanotubes alone, whereas Figure 4(b) shows the spectrum of BSA bound nanotubes, whereas Figure 4(c) shows the spectrum of the nanotubes after photopolymerization with PEGDA. Figure 4(d) shows the FTIR spectrum of PEGDA precursor by itself. The characteristic peak of the unsaturated ester C=O bond (acrylate, ~ 1722 cm^{-1})[92] in PEG-DA [Fig. 4(d)] was significantly diminished when cross-linked with BSA bound nanotubes, Figure 4(c) indicating that cross-linking has occurred on the nanotube surfaces. Further, the carbonyl peak because of amide I bonds present on the BSA bound nanotubes, which was absent in PEGDA is observed on the photopolymerized gel, further confirming the formation of PEGDA-BSA-hydrogel bound nanotubes. In addition, the peak position of the C=O amide peak changed from 1632 to 1652 cm^{-1}, further indicating interactions with the BSA moiety. The characteristic ether group peak at 1120 cm^{-1} is also observed in PEGDA and the photopolymerized sample. These results confirm the incorporation of BSA on the nanotubes as well as the formation of hydrogels on the nanotube surfaces.

Fluorescence spectroscopy

Fluorescence spectroscopic analyses were conducted to confirm the incorporation of the photoinitiator onto the BSA bound nanotubes. As shown in
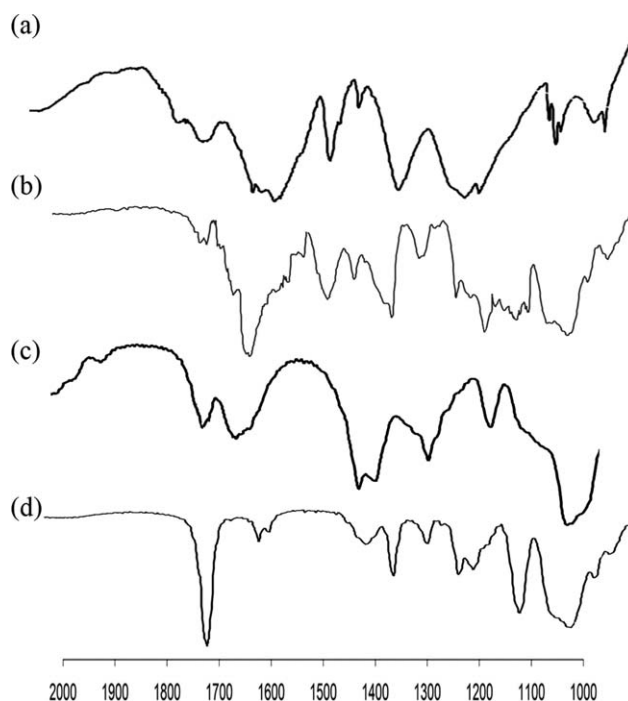
Figure 4 (a) FTIR spectrum of bare nanotubes; (b) Nanotubes bound to BSA; (c) PEGDA photopolymerized on BSA bound nanotubes; (d) PEGDA alone.
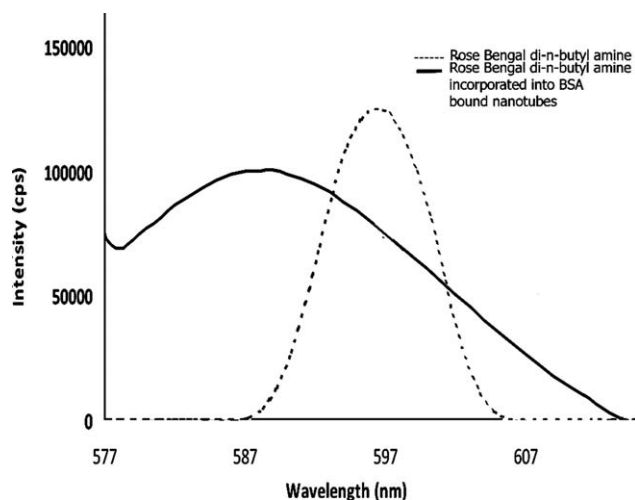
Figure 5 Comparison of fluorescence spectra of Rose Bengal di-*n*-butylamine photoinitiator before and after binding to BSA functionalized nanotubes.

Figure 5, we observed that upon incorporation, the characteristic peak of the photoinitiator (592 nm) was blue-shifted to 587 nm. Further, we also observed fluorescence quenching. The spectral blue shift of the fluorescence demonstrated here is similar to the spectral blue shift because of the dynamic Stokes shift which has been observed for dyes of the xanthene family at low temperatures or when there is change in the viscosity of the systems. In the case of nanotubes, the hypsochromic shift and quenching observed is most likely because of binding caused by electrostatic as well as hydrophobic interactions of the photoinitiator with the nanotubes indicating noncovalent binding.[93–95] These results confirm the incorporation of the photoinitiator to the nanotubes.

## Evaluation of BSA release after hydrogel formation

To evaluate the stability of the materials formed, and examine if there was any undesirable release of the BSA from the nanotubes after photopolymerization and hydrogel formation, we conducted BSA release studies. As the BSA was covalently bound to the nanotubes before photopolymerization, we did not expect BSA leaching to occur. Nevertheless we conducted these studies, to ascertain that the highly crosslinked materials formed were indeed stable for uses in various applications. Figure 6 shows the BSA release studies conducted over a period of 24 h. The amount of BSA was quantified by the Bradford method. As seen in the Figure 6, less than 4% of BSA was released, initially within the first 80 min, after which no release was observed. These results indicate that the nanotube bound BSA-PEGDA hydrogels formed were stable. The small amount of release of BSA that occurred, may be due to excess

BSA or crosslinks that may have been unbound to the nanotubes in the solution.

Thermal analyses

To examine the thermal properties of the hydrogel nanotubes obtained by photopolymerization, DSC analyses were carried out. The thermograms of dry hydrogel nanotubes (both in the presence and absence of BSA) were compared and are represented in Figure 7. In the case of nanotubes, which were bound to BSA before photopolymerization [Fig 7(a)], the DSC scan shows an endothermic step change (–22.05°C) associated with the glass-rubber transition as well as an exothermic peak (–52.15°C), which corresponds to the cold crystallization. This indicates that some of the polymer chains did not exhibit a crystalline order, whereas some had the mobility to organize into a crystalline phase. The endothermic peak observed at higher temperature is attributed to crystal melting. The shape of this peak also shows the presence of a shoulder, that may be because of the slow rate of evaporation of residual bound water that may have been present in the sample.[96] Thus overall, the materials obtained are partly crystalline. A high degree of crystallinity is not displayed most likely due to the cross-links formed with protein bound nanotubes. The crystalline phase formed in these materials primarily comprises ethylene oxide segments of PEGDA.[97] The enthalpy associated with crystal melting was determined to be 295 J/g.

On the other hand, the thermogram obtained for hydrogels prepared with nanotubes that were not bound to BSA [Fig. 7(b)] shows a single endothermic peak at higher temperature indicating crystal melting. This result shows that the hydrogels prepared with nanotubes alone display a higher degree of crystallinity compared with those obtained with BSA
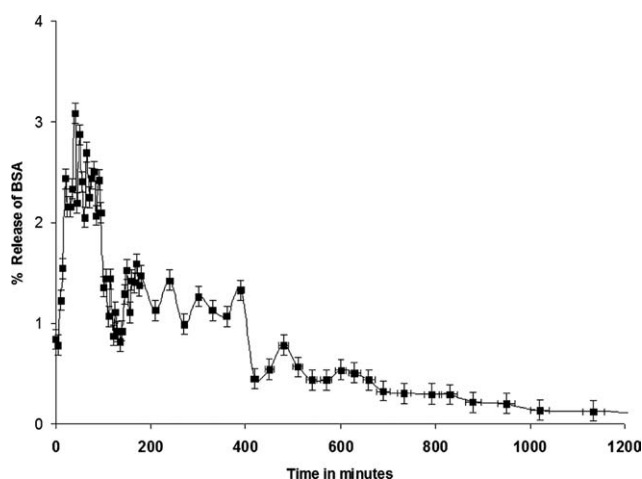
Figure 6 BSA release studies from hydrogels formed after 15 minutes of irradiation.
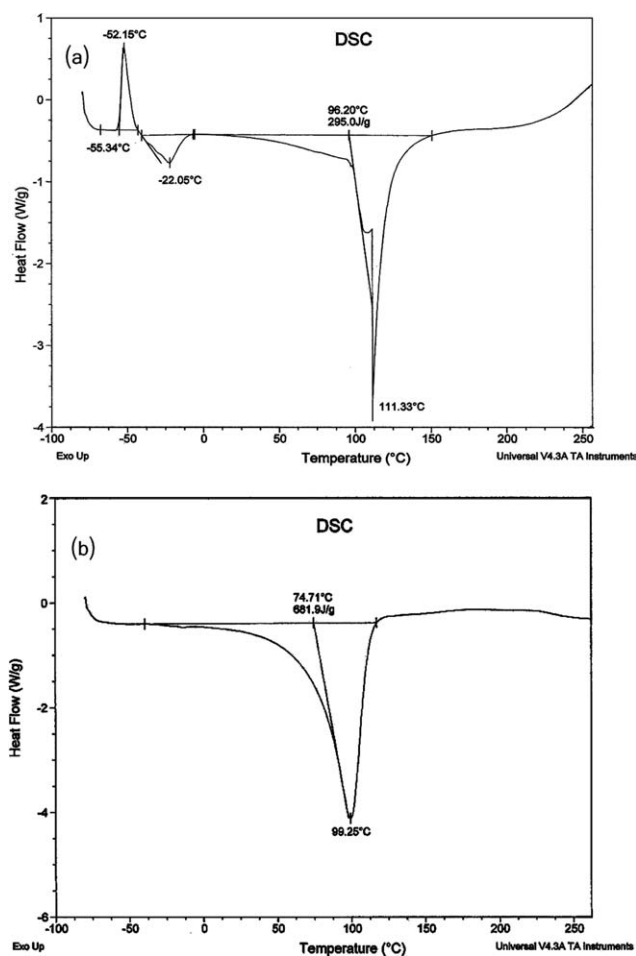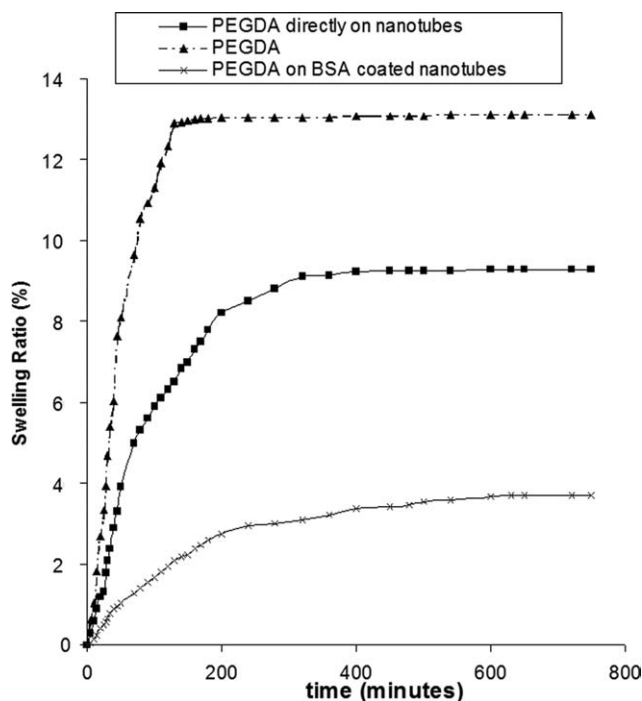
Figure 7 Comparison of DSC thermograms of hydrogels obtained on (a) BSA bound nanotubes and (b) nanotubes.

Swelling studies

Figure 8 shows the swelling kinetics of nanotube bound hydrogels in phosphate buffer saline at room temperature over a period of 12 h. Generally, both types of hydrogels (PEGDA photopolymerized on nanotubes directly and those that were photopolymerized on nanotubes bound to BSA) swelled in distilled water rapidly during the first 3 h; following which, the swelling rates of the hydrogels became relatively slower and they finally reached their swelling equilibrium in $\sim$ 10 h. As a control, we also carried out photopolymerization of 25% w/v of PEGDA alone in the presence of the photoinitiator. Because of high degree of cross-linking the equilibrium swelling ratio (Q_{eq}) value was observed to be the lowest in the case of BSA bound nanotubes. This is most likely due to relatively higher hydrophobicity of the protein bound nanotubes incorporated within the networks. It was observed that PEGDA alone has a very high Q_{eq} value because of the absence of peptide nanotubes (with or without BSA), and thus has a higher hydrophilic content compared to the nanotube bound gels. The BSA-bound nanotubes photopolymerized with PEGDA had a Q_{eq} value of 3.70%, whereas the PEGDA bound nanotubes had a relatively higher Q_{eq} value 9.20%. As expected the highest Q_{eq} values were observed in the absence of nanotubes, for PEGDA alone

bound nanotubes. It is interesting to note that no cold crystallization exotherm was observed in this case, most likely because crystallization may have occurred during the initial cooling step of the DSC procedure, thus restricting further cold crystallization during the DSC run. The enthalpy associated with crystal melting was determined to be 681.9 J/g, which is substantially higher than that obtained for hydrogels with BSA bound nanotubes. Similar trends in enthalpy associated with crystallization have been observed for poly(ε-caprolactone-polysaccharide blends).[98,99] The decrease in enthalpy in the presence of BSA bound nanotubes is mostly likely because of high degree of hydrogen bonding interactions as well as hydrophobic interactions between the components of the hydrogels and the inability to form a highly crystalline structure. Thus, the incorporation of BSA into the nanotubes before the photopolymerization of PEGDA modifies the crystalline structure as well as the hydrophilicity of the nanotube hydrogels.

Figure 8 Comparison of swelling studies of hydrogels formed by irradiation of PEGDA in the absence of nanotubes; BSA bound nanotubes; and nanotubes which were not bound to BSA prior to irradiation. In all cases, the period of irradiation was carried out for 15 minutes.

(13.08%). This indicates that crosslinking with the nanotube-bound BSA reduces hydrophilicity of the hydrogels significantly, resulting in lower water uptake. Generally, too much system water uptake or swelling may not be advantageous, as it may unfavorably affect the degradation rate.[100] Thus, swelling rates can be controlled depending upon the amount of crosslinking, which in turn depends upon the irradiation time period and concentrations of protein bound nanotubes used.

CONCLUSIONS

Peptide nanotubes were used as templates for the growth of poly(ethylene glycol) diacrylate based hydrogels via photopolymerization. Rose Bengal di-*n*-butylamine derivative was incorporated on BSA bound nanotubes, as well as on nanotubes without prior functionalization with BSA. Photopolymerization of PEGDA on the nanotube surfaces was carried out in the presence of visible light. The photoinitiator used incorporates the photoactivator dye moiety as well as the coinitiator within a single molecule, thus enhancing photopolymerization efficiency. It was observed that the swelling of the hydrogel nanotubes as well as the morphologies and extent of crosslinking varied based on whether or not BSA was bound to the nanotubes. The thermal properties of the nanocomposite hydrogels formed in the presence and absence of proteins were investigated using DSC analyses. The morphologies were examined using, SEM and AFM analyses. This mild and low cost method could be potentially applicable for the preparation of nanoscale hydrogels with a wide range of protein bound nanotubes. Such nanocomposites could be extremely efficient as three-dimensional peptide nanotube grafted scaffolds for tissue engineering applications, as well as for wound dressing materials.

References

1. Stupp, S. I.; Braun, P. V. Science 1997, 277, 1242.
2. Kay, S.; Thapa, A.; Haberstroh, K. M.; Webster, T. J. Tissue Eng 2002, 8, 753.
3. Hong, Z.; Zhang, P.; He, C.; Qiu, X.; Liu, A.; Chen, L.; Chen, X.; Jing, X. Biomaterials 2005, 26, 32.
4. Thomas, V.; Dean, D. R.; Vohra, Y. K. Curr Nanosci 2006, 2, 155.
5. Barbucci, R.; Pasqui, D.; Wirsen, A.; Affrossman, S.; Curtis, A.; Tetta, C. J Mater Sci Mater Med 2003, 14, 721.
6. Kwon, I. K.; Kidoaki, S.; Matsuda, T. Biomaterials 2005, 26, 3929.
7. Mills, C. A.; Escarré, J.; Engel, E.; Martinez, E.; Errachid, A.; Bertomeu, J.; Andreu, J.; Planell, J. A.; Samitier, J. Nanotechnology 2005, 16, 369.
8. Dai, L.; Mau, A. W. H. J Phys Chem B 2000, 104, 1891.
9. Abidian, M. R.; Martin, D. C. Adv Funct Mater 2009, 19, 573.
10. Kim, M. S.; Seo, K. S.; Khang, G.; Lee, H. B. Langmuir 2005, 21, 4066.
11. Sanhvi, A. B.; Miller, K. P.-H.; Belcher, A. M.; Schmidt, C. E. Nat Mater 2005, 4, 496.
12. Ma, Z.; Kotaki, M.; Yong, T.; He, W.; Ramakrishna, S. Biomaterials 2005, 26, 2527.
13. Stolnik, S.; Dunn, S. E.; Garnett, M. C.; Davies, M. C.; Coombes, A. G.; Taylor, D. C.; Irving, M. P.; Purkiss, S. C.; Tadros, T. F.; Davis, S. S.; Illum, L. Pharm Res 1994, 11, 1800.
14. Tiwari, A.; Singh, S. P. J Appl Polym Sci 2008, 108, 1169.
15. Andrade, G.; Barbosa-Stancioli, E. F.; Mansur, A. A. P.; Vasconcelos, W. L.; Mansur, H. S. Biomed Mater 2006, 1, 221.
16. Khor, E.; Li, H. C.; Wee, A. Biomaterials 1996, 17, 1877.
17. Schiraldi, C.; D'agostino, A.; Oliva, A.; Flamma, F.; De Rosa, A.; Apicella, A.; Aversa, R.; De Rosa, M. Biomaterials 2004, 25, 3645.
18. Kim, W.-S.; Kim, M.-G.; Ahn, J.-H.; Bae, B.-B.; Park, C. B. Langmuir 2007, 23, 4732.
19. Loschonsky, S.; Shroff, K.; Wörz, A.; Prucker, O.; Rühe, J.; Biesalski, M. Biomacromolecules 2008, 9, 543.
20. Tian, D.; Blacher, S.; Pirard, J.-P.; Jérôme, R. Langmuir 1998, 14, 1905.
21. Numata, M.; Hasegawa, T.; Fujisawa, T.; Sakurai, K.; Shinkai, S. Org Lett 2004, 6, 4447.
22. Pennadam, S. S.; Firman, K.; Alexander, C.; Górecki, D. C. J Nanobiotechnol 2004, 2, 8.
23. Bachelder, E. M.; Beaudette, T. T.; Broaders, K. E.; Dashe, J.; Fréchet, J. M. J Am Chem Soc 2008, 130, 10494.
24. Alemdaroglu, F. E.; Herrmann, A. Org Biomol Chem 2007, 5, 1311.
25. Gayet, J. C.; Fortier, G. J. Control Release 1996, 38, 177.
26. Langer, R.; Tirrell, D. A. Nature 2004, 428, 487.
27. Vandermeulen, G. W. M.; Klok, H.-A. Macromol Biosci 2004, 4, 383.
28. Castelvetro, V.; De Vita, C. Adv Colloid Interface Sci 2004, 108, 167.
29. Greiner, A.; Wendroff, J. H.; Yarin, A. L.; Zussman, E. Appl Microbiol Biotechnol 2006, 71, 387.
30. Gill, I. Chem Mater 2001, 13, 3404.
31. Metzke, M.; O'Connor, N.; Maiti, S.; Nelson, E.; Guan, Z. Angew Chem Int Ed 2005, 44, 6529.
32. Gillies, E. R.; Dy, E.; Fréchet, J. M. J.; Szoka, F. C. Mol Pharm 2005, 2, 129.
33. Rahman, M. A.; Kumar, P.; Park, D.-S.; Shim, Y.-B. Sensors 2008, 8, 118.
34. Hamidi, M.; Azadi, A.; Rafiei, P. Adv Drug Deliv Rev 1638, 60, 2008.
35. Peppas, N. A.; Bures, P.; Leobandung, W.; Ichikawa, H. Eur J Pharm Biopharm 2000, 50, 27.
36. Cohn, D.; Sosnik, A.; Garty, S. Biomacromolecules 2005, 6, 1168.
37. Luchini, A.; Geho, D. H.; Bioshop, B.; Tran, D.; Xia, C.; Dufour, R. L.; Jones, C. D.; Espina, V.; Patanarut, A.; Zhou, W.; Ross, M. M.; Tessitore, A.; Petricoin, E. F.; Liotta, A. Nano Lett 2008, 8, 350.
38. Madsen, J.; Armes, S. P.; Bertal, K.; Lomas, H.; Macneil, S.; Lewis, A. L. Biomacromolecules 2008, 9, 2265.
39. Ichikawa, H.; Fukumori, Y. J. Control Release 2000, 63, 107.
40. Huang, X.; Lowe, T. T. Biomacromolecules 2005, 6, 2131.
41. Ishihara, M.; Obara, K.; Ishizuka, T.; Fujita, M.; Sato, M.; Masuoka, K.; Saito, Y.; Yua, H.; Matsui, T.; Hattori, H.; Kikuchi, M.; Kurita, A. J Biomed Mater Res A 2003, 64, 551.
42. Gulsen, D.; Chauhan, A. Int J Pharm 2005, 292, 95.

43. Chen, X.; Dunn, A. C.; Sawyer, W. G.; Sarntinoranont, M. J Biomech Eng 2007, 129, 156.
44. Fenglan, X.; Yubao, L.; Xuejiang, W.; Jie, W.; Aiping, Y. J Mater Sci 2004, 39, 5669.
45. Lin, C.-C.; Metters, A. T. Pharm Res 2006, 23, 614.
46. Yuan, J.-J.; Jin, R.-H. Langmuir 2005, 21, 3136.
47. Rice, C. V. Biomacromolecules 2006, 7, 2923.
48. Oh, K. T.; Bronich, T. K.; Kabanov, V. A.; Kabanov, A. V. Biomacromolecules 2007, 8, 490.
49. Da Silveira, B. I. Eur Polym J 1993, 29, 1095.
50. Wan, W. K.; Campbell, G.; Zhang, Z. F.; Hui, A. J.; Boughner, D. R. J Biomed Mater Res B 2002, 63, 854.
51. Hyon, S. H.; Cha, W. I.; Ikada, Y.; Kita, M.; Ogura, Y.; Honda, Y. J Biomater Sci Polym Ed 1994, 5, 397.
52. Peppas, N. A.; Keys, K. B.; Torres-Lugo, M.; Lowman, A. M. J. Control Release 1999, 62, 81.
53. Raeber, G. P.; Lutolf, M. P.; Hubbell, J. A. Biophys J 2005, 89, 1374.
54. Dimitrov, M.; Lambov, N.; Shenkov, S.; Dosseva, V.; Baranovski, V. Y. Acta Pharm 2003, 53, 25.
55. Park, Y. D.; Tirelli, N.; Hubbell, J. A. Biomaterials 2003, 24, 893.
56. Han, D. K.; Hubbell, J. A. Macromolecules 1997, 30, 6077.
57. Desai, N. P.; Sojomihardjo, A.; Yao, Z.; Ron, N.; Soon-Shiong, P. J Microencapsul 2000, 17, 677.
58. Zhang, L.; Xiong, C.; Deng, X. J Appl Polym Sci 1995, 56, 103.
59. Ge, H.; Hu, Y.; Jiang, X.; Cheng, D.; Yuan, Y.; Bi, H.; Yang, C. J Pharm Sci 2002, 91, 1463.
60. Kommareddy, S.; Amiji, M. J Pharm Sci 2007, 96, 397.
61. Halstenberg, S.; Panitch, A.; Rizzi, S.; Hall, H.; Hubbell, J. A. Biomacromolecules 2002, 3, 710.
62. Dadsetan, M.; Szatkowski, J. P.; Yaszemski, M. J.; Lu, L. Biomacromolecules 2007, 8, 1702.
63. Hong, Y.; Krsko, P.; Libera, M. Langmuir 2004, 20, 11123.
64. An, S. Y.; Bui, M.-P.; Nam, Y. J.; Han, K. N.; Li, C. A.; Choo, J.; Lee, E. K.; Katoh, S.; Kumada, Y.; Seong, G. H. J Colloid Interface Sci 2009, 331, 98.
65. Shim, M.; Kam, N. W. S.; Chen, R. J.; Li, Y.; Dai, H. Nano Lett 2002, 2, 285.
66. Coyet, J.; Jeyaprakash, J. D.; Samuel, S.; Kopyshev, A.; Santer, S.; Biesalski, M. Angew Chem Int Ed 2005, 44, 3297.
67. Kol, N.; Adler-Abramovich, L.; Barlam, D.; Shneck, R. Z.; Gazit, E.; Rousso, I. Nano Lett 2005, 5, 1343.
68. Subramani, K.; Khraisat, K.; George, A. Curr Nanosci 2008, 4, 207.
69. Martin, C. R.; Kohli, P. Nat Rev Drug Discov 2003, 2, 29.
70. Santoso, S. S.; Vauthey, S.; Zhang, S. Curr Opin Colloid Interface Sci 2002, 7, 262.
71. Fairman, R.; Akerfeldt, K. S. Curr Opin Struct Biol 2005, 15, 453.
72. Kohli, P.; Martin, C. R. Curr Pharm Biotechnol 2005, 6, 35.
73. Hartgerink, J. D.; Granja, J. R.; Milligan, R. A.; Ghadiri, M. R. J Am Chem Soc 1996, 118, 43.
74. Gao, X. Y.; Matsui, H. Adv Mater 2005, 17, 2037.
75. Amiji, M.; Park, K. J Biomater Sci Polym Ed 1993, 4, 217.

76. Spear, R. L.; Tamayev, R.; Fath, K. R.; Banerjee, I. A. Colloid Surf B 2007, 60, 158.
77. Menzenski, M. Z.; Banerjee, I. A. New J Chem 2007, 31, 1674.
78. Kogiso, M.; Ohnishi, S.; Yase, K.; Masuda, M.; Shimizu, T. Langmuir 1998, 14, 4978.
79. Banerjee, I. Photochemistry and Applications of Protein-Bound Dyes and Dye-Amine Conjugates in the Presence of Visible Light, Ph.D. thesis, University of Connecticut, 2001.
80. Sereikaite, J.; Bumeliene, Z.; Bumelis, V. A. Acta Chromatogr 2005, 15, 298.
81. Waheed, A. A.; Rao, K. S.; Gupta, P. D. Anal Biochem 2000, 287, 73.
82. Pérez-Ruiz, T.; Martínez-Lozano, C.; Tomás, V.; Fenoll, J. Analyst 2000, 125, 507.
83. Matsui, H. In Encyclopedia of Nanoscience and Nanotechnology, Nalwa, H. S., Ed.; American Scientific Publishers: Stevenson Ranch, CA, 2004; Chapter 8, p 445.
84. Feitelson, M. A.; Wettstein, F. O.; Stevens, J. G. Anal Biochem 1981, 116, 473.
85. Abuin, E.; Aspee, A.; Lissi, E.; Leon, L. J Chil Chem Soc 2007, 52, 1196.
86. Encinas, M. V.; Rufs, A. M.; Bertolotti, S. G.; Previtali, C. M. Polymer 2009, 50, 2762.
87. Campagnola, P. J.; Delguidice, D. M.; Epling, G. A.; Hoffacker, K. D.; Howell, A. R.; Pitts, J. D.; Goodman, S. L. Macromolecules 2000, 33, 1511.
88. Manivannan, G.; Leclere, P.; Semal., S.; Changakakoti, R.; Renotte, Y.; Lion, Y.; Lessard, R. A. Appl Phys B: Lasers Opt 1994, 58, 73.
89. Kizilel, S.; Pérez-Luna, V. H.; Teymour, F. Langmuir 2004, 20, 8652.
90. Baptista, M. S.; Indig, G. L. J Phys Chem B 1998, 102, 4678.
91. Pitts, J. D.; Howell, A. R.; Taboada, R.; Banerjee, I.; Wang, J.; Goodman, S. L.; Campagnola, P. J Photochem Photobiol 2002, 76, 135.
92. Guo, K.; Chu, C. C. J Polym Sci A 2005, 43, 3932.
93. Nizomov, N.; Ismailov, Z. F.; Nizamov, S. N.; Salakhitdinova, M.; Tatrets, A.; Patsenker, L. D.; Khodjayev, G. J Mol Struct 2006, 788, 36.
94. Patonay, G.; Salon, J.; Sowell, J.; Strekoswski, L. J Mol Struct 2004, 9, 40.
95. Kinoshita, S.; Nishi, N.; Kushida, T. Chem Phys Lett 1987, 134, 605.
96. Gayet, J. C.; He, P.; Fortier, G. J Bioactive Compatible Polym 1998, 13, 179.
97. Lin, H.; Vanwagner, E.; Swinnea, J. S.; Freeman, B. D.; Pas, S. J.; Hill, A. J.; Kalakkunnath, S.; Kalika, D. S. J Membr Sci 2006, 276, 145.
98. Rutot, D.; Duquesne, E.; Ydens, I.; Degee, P.; Dubois, P. Polym Degrad Stab 2001, 73, 561.
99. Chiono, V.; Vozzi, G.; D'Acunto, M.; Brinzi, S.; Domenici, C.; Vozzi, F.; Ahluwalia, A.; Barbani, N.; Giusti, P.; Ciardelli, G. Mater Sci Eng C 2009, 29, 2174.
100. Weiner, A. A.; Shuck, D. M.; Bush, J. R.; Shastri, P. Biomaterials 2007, 28, 5259.